

# Correlations of conserved number mixed susceptibilities in a hadron resonance gas model

D. K. Mishra,<sup>1,\*</sup> P. K. Netrakanti,<sup>1,†</sup> and Bedangadas Mohanty<sup>2,‡</sup>

<sup>1</sup>*Nuclear Physics Division, Bhabha Atomic Research Center, Mumbai 400085, India*

<sup>2</sup>*National Institute of Science Education and Research, Jatni 752050, India*

The ratios of off-diagonal and diagonal susceptibilities of conserved charges are studied using a hadron resonance gas (HRG) model with an emphasis towards providing a proper baseline for comparison to the corresponding future experimental measurements. We have studied the effect of kinematic acceptances, transverse momentum ( $p_T$ ) and pseudorapidity ( $\eta$ ), and different charged states on the ratios of the calculated susceptibilities. We find that the effect of  $p_T$  and  $\eta$  acceptance on the ratio of the susceptibilities are small relative to their dependence on the beam energy or the charged states of the used particles. We also present a HRG based calculation for various combinations of cumulant ratios of protons and pions, recently proposed as robust observables (with no theoretical uncertainties) for critical point search in the experiments. These results which increase as a function of collision energy will provide a better baseline for non-critical point physics compared to Poisson expectation.

PACS numbers: 25.75.Gz,12.38.Mh,21.65.Qr,25.75.-q,25.75.Nq

## I. INTRODUCTION

In recent years, beam energy scan (BES) program carried out at Relativistic Heavy-Ion Collider (RHIC) has drawn much attention with an aim to explore the quantum chromodynamics (QCD) phase diagram at non-zero temperature ( $T$ ) and baryon chemical potential ( $\mu_B$ ) [1–3]. One of the key observable is related to the event-by-event distribution of conserved charge numbers such as: net-baryon, net-electric charge and net-strangeness [4–6]. Current experiments at RHIC have reported the measurements for various order moments of net-proton and net-charge event-by-event distributions using the BES phase-I data [7–10]. From the net-proton measurement, deviations are observed for  $\sqrt{s_{NN}} \leq 27$  GeV for ratios of higher order cumulants compared to expectation from a Hadron Resonance Gas (HRG) model and Skellam statistics [8]. However, from the experimental side, there is no conclusive evidence about the location of the QCD critical end point (CEP). This has prompted to have high statistics BES-II program scheduled for 2018-19 with the focus on taking data at lower beam energies (below 39 GeV). So far, the reported experimental measurements are based on higher moments of either net-proton or net-charge multiplicity distribution, which are related to baryon number or electric charge susceptibilities, respectively [7, 11].

Probes of phase structure of QCD should also include correlations among different conserved charges [12]. They are not only expected to vary in some characteristic manner between low and high temperature phases of QCD but also provide insight into applicability of the

HRG model. It has been suggested that, the ratio of strange to non-strange susceptibilities calculated in lattice QCD can give insight about Quark Gluon Plasma (QGP) phase [13]. The correlation between baryon number ( $B$ ) and electric charge ( $Q$ ) ( $\chi_{BQ}$ ) shows a variation with the temperature which are correlated with the changes in relevant degrees of freedom [12]. At lower temperature  $\chi_{BQ}$  is dominated by contributions from protons and anti-protons, whereas in the high temperature limit of (2+1) flavor QCD, their values are due to quark degrees of freedom. Similarly, correlations of baryons with strangeness ( $\chi_{BS}$ ) and electric charge with strangeness ( $\chi_{QS}$ ) are sensitive to the strangeness degrees of freedom of the system [14, 15]. At high temperature limit, in which the basic degrees of freedom are quarks and gluons, the strangeness is carried by the  $s$  and  $\bar{s}$  quarks that later carry the baryon number in strict proportion to their strangeness number ( $B = -\frac{1}{3}S$ ) which makes the  $B$  and  $S$  strongly correlated [14]. On the other hand, in a hadron gas the strangeness is mostly carried by kaons with  $B \approx 0$ , which makes the correlation between strangeness and baryon number very small. Hence, observables such as  $\chi_{QS}$ ,  $\chi_{BQ}$  and  $\chi_{BS}$  give information about the QCD phase structure [12].

Further, combinations of diagonal and off-diagonal quark number susceptibilities can be used to obtain the fluctuations of conserved charges [16–18]. Diagonal susceptibilities measure the quark number density to changes in  $T$  and  $\mu_B$ . At high temperature region diagonal susceptibilities show large values and expected to approach the ideal gas limit [18]. Whereas in the low temperature region, the quarks are confined, the diagonal susceptibilities are expected to have small values. The off-diagonal susceptibilities in turn can be used to explore the degree of correlation between different charge and baryon numbers that carry different flavors [16–18]. Using the ratio of susceptibilities,  $\chi_{BS}/\chi_S$  and  $\chi_{QS}/\chi_S$ , it has been observed that, above critical temperature

\*Electronic address: dkmishra@rcf.rhic.bnl.gov

†Electronic address: pawannetrakanti@gmail.com

‡Electronic address: bedanga@niser.ac.in

( $T_c$ ), the flavor carrying sector of QCD is consistent with deconfined plasma of weakly interacting quarks and anti-quarks. Above  $1.5T_c$ , the flavor carrying degrees of freedom are quark-like quasi-particles. Below  $T_c$  the behavior of the above susceptibility ratios is consistent with that of hadron resonance gas [15].

In addition, a landmark point in the QCD phase diagram is the CEP [19, 20]. As one approaches the CEP in the phase diagram, there will be large fluctuations in the event-by-event produced particle numbers [21]. These fluctuations are quantified by measuring various order moments of the event-by-event particle number distribution. These moments are related to some power of correlation length ( $\xi$ ) of the system [19, 22–24]. Higher moments of the distributions are related to the higher power of  $\xi$  which makes them more sensitive to CEP effects [5, 25]. Specifically it has been recently suggested to look for mixed pion-proton cumulants as a signature for CEP [21]. The paper suggests to construct five specific mixed pion-proton cumulants from which when non-CEP contributions are subtracted will yield a value of unity if the system experiences critical phenomena. Such ratios have no theoretical uncertainties arising from uncertainty in the values of the QCD based parameters. These ratios are claimed to provide strong evidence needed for the discovery of the QCD critical point.

Keeping in mind above aspects and the importance of having a proper baseline for the experimental measures, we discuss in the present paper, mixed susceptibilities (between electric charge, baryon number, and strangeness) and various order pion-proton cumulants within the frame work of a HRG model [26–28]. The calculations presented here also keeps in mind the actual experimental situation in terms of acceptances (in momentum and rapidity) and measurable quantities [29, 30].

The paper is organized as follows. In the following section, we discuss the HRG model used in this study. In Section III, the results for various mixed cumulants are presented for different kinematic acceptance and charge states. In Section IV, we present the proper baseline for critical fluctuation. Finally in Section V, we summarize our findings and mention about the implications of this work in current experimental measurements in high energy heavy-ion collisions.

## II. MIXED SUSCEPTIBILITIES IN HADRON RESONANCE GAS MODEL

The partition function ( $Z$ ) in the HRG model include all the degrees of freedom of confined, strongly interacting matter and implicitly contains all the interactions that result in resonance formation [31]. The logarithm of the partition function is given by

$$\ln Z(T, \mu, V) = \sum_M \ln Z_i(T, \mu_i, V) + \sum_B \ln Z_i(T, \mu_i, V) \quad (1)$$

where

$$\ln Z_i(T, \mu_i, V) = \pm \frac{V g_i}{2\pi^2} \int d^3 p \ln \{1 \pm \exp[(\mu_i - E)/T]\}, \quad (2)$$

$T$  is the temperature,  $V$  is the volume of the system,  $\mu_i$  is the chemical potential and  $g_i$  is the degeneracy factor of the  $i^{\text{th}}$  particle. The total chemical potential  $\mu_i = B_i \mu_B + Q_i \mu_Q + S_i \mu_S$ , where  $B_i$ ,  $Q_i$  and  $S_i$  are the baryon, electric charge and strangeness number of the  $i^{\text{th}}$  particle, with corresponding chemical potentials  $\mu_B$ ,  $\mu_Q$  and  $\mu_S$ , respectively. The *+*ve and *-*ve signs are for baryons and mesons respectively. The thermodynamic pressure ( $P$ ) can then be obtained from the logarithm of partition function in the limit of large volume as:

$$P(T, \mu_i, V) = \frac{T}{V} \ln Z_i = \pm \frac{T g_i}{2\pi^2} \int d^3 k \ln \{1 \pm \exp(\mu_i - E)/T\} \quad (3)$$

In a static fireball, a particle of mass  $m$  with  $p_T$ ,  $\eta$  and  $\phi$  as the transverse momentum, pseudo-rapidity and azimuthal angle, respectively, the volume element ( $d^3 p$ ) and energy ( $E$ ) of the particle can be written as  $d^3 p = p_T m_T \cosh \eta dp_T d\eta d\phi$  and  $E = m_T \cosh \eta$ , where  $m_T$  is the transverse mass  $= \sqrt{m^2 + p_T^2}$ . The experimental acceptances can be applied by considering the corresponding ranges in  $p_T$ ,  $\eta$  and  $\phi$  [29]. The fluctuations of the conserved numbers are obtained from the derivative of the thermodynamic pressure with respect to the corresponding chemical potentials  $\mu_B$ ,  $\mu_Q$  or  $\mu_S$ . The  $n$ -th order generalized susceptibilities ( $\chi_x$ ), where  $x$  represents baryon, electric charge or strangeness indices, can be expressed as;

$$\chi_x^n = \frac{d^n [P(T, \mu)/T^4]}{d(\mu_x/T)^n} \quad (4)$$

For mesons  $\chi_x$  can be expressed as

$$\chi_{x,meson}^{(n)} = \frac{X^n}{VT^3} \int d^3 p \sum_{k=0}^{\infty} (k+1)^{n-1} \times \exp\left\{\frac{-(k+1)E}{T}\right\} \exp\left\{\frac{(k+1)\mu}{T}\right\}. \quad (5)$$

and for baryons,

$$\chi_{x,baryon}^{(n)} = \frac{X^n}{VT^3} \int d^3 p \sum_{k=0}^{\infty} (-1)^k (k+1)^{n-1} \times \exp\left\{\frac{-(k+1)E}{T}\right\} \exp\left\{\frac{(k+1)\mu}{T}\right\}, \quad (6)$$

where  $X$  represents either  $B_i$ ,  $Q_i$  or  $S_i$  of the  $i$ -th particle. The total generalized susceptibilities will be the sum of susceptibility of mesons and baryons as  $\chi_x^n = \sum \chi_{x,mesons}^n + \sum \chi_{x,baryons}^n$ . Further, the mixed susceptibilities of the correlated conserved charges can be obtained by taking the derivative of the pressure with re-

spect to different chemical potentials for conserved quantities  $X$  and  $Y$ ,

$$\chi_{xy}^{(n,m)} = \frac{d^{n+m}[P(T, \mu)/T^4]}{d(\mu_x/T)^n d(\mu_y/T)^m} \quad (7)$$

where  $m$  and  $n$  correspond to the different order of derivatives,  $x$  and  $y$  are baryon–electric charge, baryon–strangeness or electric charge–strangeness mixed indices and  $X, Y$  are combinations of either  $B, Q$  or  $S$ . Hence, Eq. 5 and 6 can be written as:

$$\chi_{xy,meson}^{(n,m)} = \frac{X^n Y^m}{VT^3} \int d^3p \sum_{k=0}^{\infty} (k+1)^{n-1} (k+1)^{m-1} \times \exp\left\{\frac{-(k+1)E}{T}\right\} \exp\left\{\frac{(k+1)\mu}{T}\right\}, \quad (8)$$

and

$$\chi_{xy,baryon}^{(n,m)} = \frac{X^n Y^m}{VT^3} \int d^3p \sum_{k=0}^{\infty} (-1)^k (k+1)^{n-1} (k+1)^{m-1} \times \exp\left\{\frac{-(k+1)E}{T}\right\} \exp\left\{\frac{(k+1)\mu}{T}\right\}. \quad (9)$$

Using Eq. 8 and 9, one can calculate the conserved charge correlations in the HRG model. The freeze-out parameters used in the HRG are extracted from a statistical model description of particle yields. The parametrization of  $\mu_B$  and  $T$  as a function collision energies ( $\sqrt{s_{NN}}$ ) are given in [27, 31]. Other effects like collective flow and resonances on susceptibilities are discussed in Ref. [29].

### III. ACCEPTANCE EFFECT ON CORRELATED SUSCEPTIBILITIES

The phase structure of QCD at finite temperature and baryon chemical potential can be probed using correlation among different conserved charges. There are significant changes of these correlations in the crossover region between the low and high temperature phases of QCD [12]. As one goes from low to high temperature phase, it is expected that there is change in correlations between baryon number and electric charge ( $\chi_{BQ}$ ), between baryon number and strangeness number ( $\chi_{BS}$ ), also between strangeness number and electric charge ( $\chi_{QS}$ ). In the following subsections, we discuss the effect of kinematic acceptances in the various mixed susceptibilities of the conserved charges. In the present study we have considered  $\chi_{BQ}^{11}/\chi_B^2$ ,  $\chi_{BQ}^{11}/\chi_Q^2$ ,  $\chi_{QS}^{11}/\chi_Q^2$ ,  $\chi_{QS}^{11}/\chi_S^2$ ,  $\chi_{BS}^{11}/\chi_B^2$  and  $\chi_{BS}^{11}/\chi_S^2$ , ratios. The numerator in the first two ratios ( $\chi_{BQ}^{11}/\chi_B^2$  and  $\chi_{BQ}^{11}/\chi_Q^2$ ) receive contributions only from charged baryons and anti-baryons (i.e. particles starting from protons to all higher mass charged baryons), where as the denominator receives contributions from all baryons or all charge particles. In

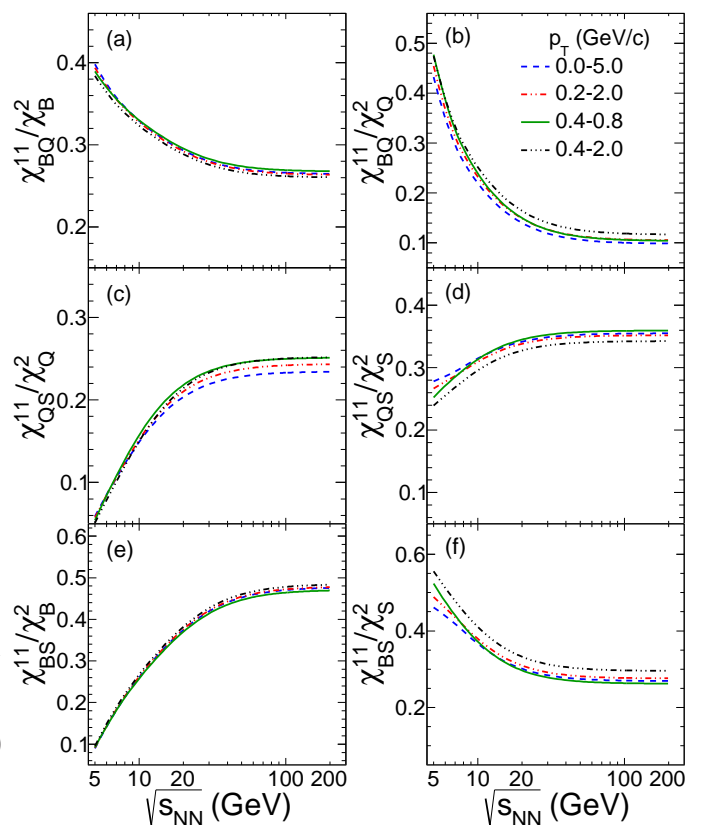


FIG. 1: Ratios of diagonal susceptibility to second order susceptibility ( $\chi_{xy}^{11}/\chi_{x,y}^2$ ) as a function of  $\sqrt{s_{NN}}$  within  $|\eta| \leq 0.5$  from the HRG model, where  $x$  and  $y$  stand for either  $B, Q$  or  $S$ . Panels (a) and (b) shows the diagonal susceptibility ratios for charged baryons. Panels (c) and (d) shows the diagonal susceptibility ratios for charged particles with at least one strange quark. Panels (e) and (f) shows the diagonal susceptibility ratios for baryons with strange quark. The ratios are also compared for various  $p_T$  acceptance ranges.

case of other two ratios ( $\chi_{QS}^{11}/\chi_Q^2$  and  $\chi_{QS}^{11}/\chi_S^2$ ), the numerators receive contributions from charged strange and anti-strange particles, with kaon being the first charged strange particle, where as denominators receive contributions from all charged or strange particles, respectively. Similarly, in case of ratios ( $\chi_{BS}^{11}/\chi_B^2$  and  $\chi_{BS}^{11}/\chi_S^2$ ), the numerators receive contributions from strange baryons (anti-baryons), with particle starting from  $\Lambda^0$  and higher masses of strange baryons, where as denominators receive contributions from all baryons or strange particles. It is to be noted that, in real experimental situation, it may be difficult to measure the strange baryons on an event-by-event basis and calculate their cumulants for studying the fluctuations. Particularly, at lower collision energies, where the strange baryon production is very small, the above observable will be difficult to measure experimentally.

### A. Effect of $p_T$ acceptance

Figure 1 shows the variation of  $\chi_{BQ}^{11}/\chi_B^2$ ,  $\chi_{BQ}^{11}/\chi_Q^2$ ,  $\chi_{QS}^{11}/\chi_Q^2$ ,  $\chi_{QS}^{11}/\chi_S^2$ ,  $\chi_{BS}^{11}/\chi_B^2$ , and  $\chi_{BS}^{11}/\chi_S^2$  ratios as a function of  $\sqrt{s_{NN}}$  for different  $p_T$  acceptances. There is small  $p_T$  dependence of the above ratios. However, there is a strong energy dependence for  $\chi_{BQ}^{11}/\chi_Q^2$ ,  $\chi_{QS}^{11}/\chi_Q^2$ , and  $\chi_{BS}^{11}/\chi_B^2$  ratios. Figure 2 shows the corresponding ra-

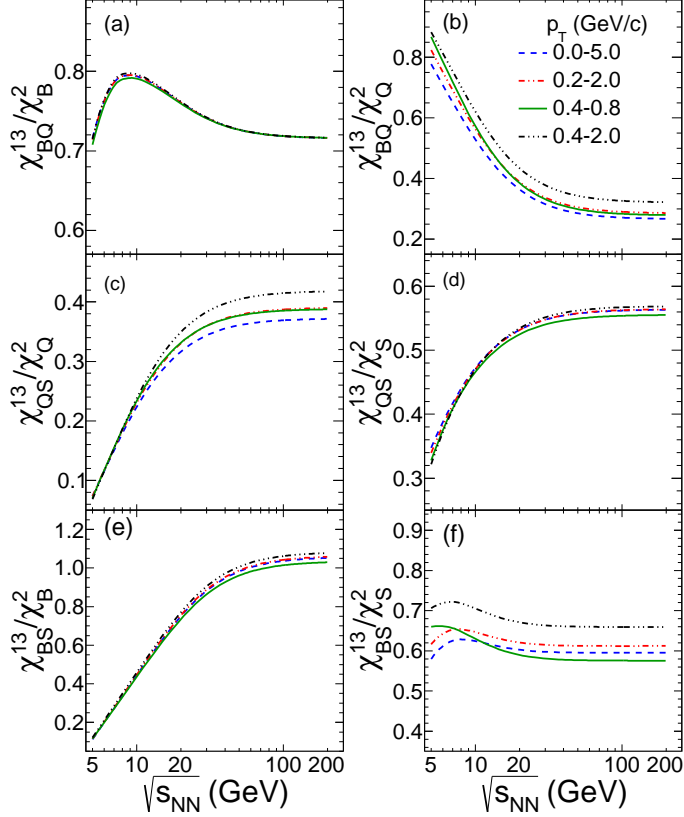


FIG. 2: Ratios of off-diagonal susceptibility to second order susceptibility ( $\chi_{xy}^{13}/\chi_{x,y}^2$ ) as a function of  $\sqrt{s_{NN}}$  within  $|\eta| \leq 0.5$  from HRG, where  $x$  and  $y$  stand for either  $B$ ,  $Q$  or  $S$ . Panels (a) and (b) shows the off-diagonal susceptibility ratios for charged baryons. Panels (c) and (d) shows the off-diagonal susceptibility ratios for charged particles with at least one strange quark. Panels (e) and (f) shows the off-diagonal susceptibility ratios for baryons with strange quark. The ratios are also compared for various  $p_T$  acceptance ranges.

tios for off-diagonal susceptibilities ( $\chi_{BQ}^{13}/\chi_Q^2$ ,  $\chi_{BQ}^{13}/\chi_B^2$ ,  $\chi_{QS}^{13}/\chi_Q^2$ ,  $\chi_{QS}^{13}/\chi_S^2$ ,  $\chi_{BS}^{13}/\chi_B^2$ , and  $\chi_{BS}^{13}/\chi_S^2$ ) as a function of  $\sqrt{s_{NN}}$ . All the ratios show stronger energy dependence when compared with the previous ratios ( $\chi^{11}/\chi^2$ ). There is a visibly  $p_T$  dependence on  $\chi_{BQ}^{13}/\chi_Q^2$ ,  $\chi_{QS}^{13}/\chi_Q^2$ , and  $\chi_{BS}^{13}/\chi_S^2$  ratios for all collision energies. The  $\chi_{BQ}^{13}/\chi_B^2$ ,  $\chi_{QS}^{13}/\chi_S^2$ , and  $\chi_{BS}^{13}/\chi_B^2$  are least affected by different  $p_T$  acceptances.

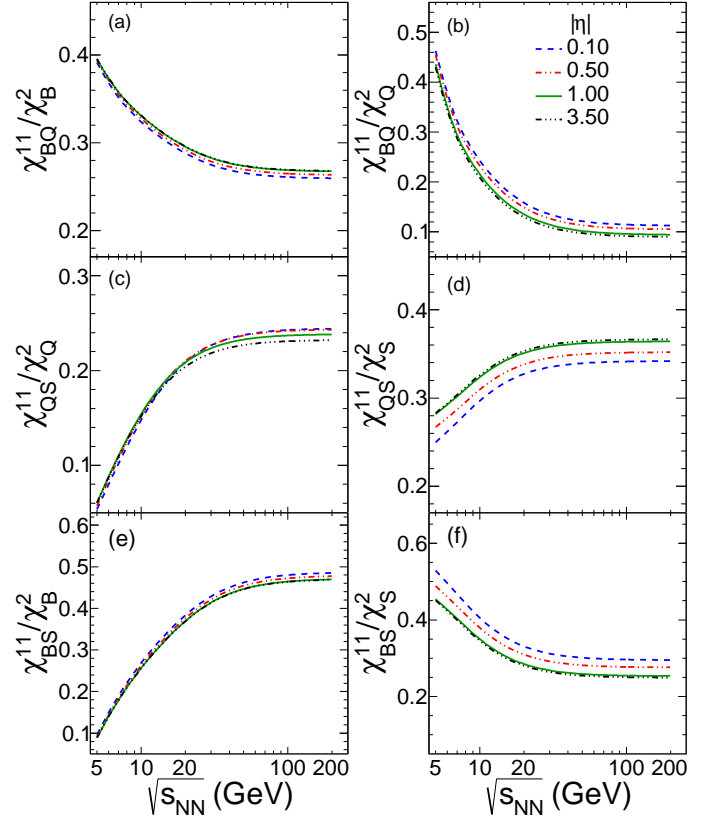


FIG. 3: Ratios of diagonal susceptibility to second order susceptibility ( $\chi_{xy}^{11}/\chi_{x,y}^2$ ) as a function of  $\sqrt{s_{NN}}$  within  $0.2 \leq p_T \text{ GeV}/c \leq 2.0$  from the HRG model, where  $x$  and  $y$  stand for either  $B$ ,  $Q$  or  $S$ . Panels (a) and (b) shows the diagonal susceptibility ratios for charged baryons. Panels (c) and (d) shows the diagonal susceptibility ratios for charged particles with at least one strange quark. Panels (e) and (f) shows the diagonal susceptibility ratios for baryons with strange quark. The ratios are also compared for various  $\eta$  acceptance ranges.

### B. Effect of $\eta$ acceptance

Figure 3 shows the variation of  $\chi_{BQ}^{11}/\chi_B^2$ ,  $\chi_{BQ}^{11}/\chi_Q^2$ ,  $\chi_{QS}^{11}/\chi_Q^2$ ,  $\chi_{QS}^{11}/\chi_S^2$ ,  $\chi_{BS}^{11}/\chi_B^2$ , and  $\chi_{BS}^{11}/\chi_S^2$  ratios as a function of  $\sqrt{s_{NN}}$  for different ranges of  $\eta$  acceptances. The  $p_T$  range for all the particles are considered within  $0.2 - 2.0 \text{ GeV}/c$ . Similar to  $p_T$  dependence, there is small  $\eta$  dependence of the above ratios. However, the  $\eta$  dependence is more visible in case of  $\chi_{QS}^{11}/\chi_S^2$  and  $\chi_{BS}^{11}/\chi_S^2$  ratios with compared to other three ratios. The  $\eta$  dependence is even higher in case of higher order mixed susceptibility ratios ( $\chi^{13}/\chi^2$ ) as a function of collision energies, which are shown in Fig. 4. There is no effect of  $\eta$  acceptances on the  $\chi_{BQ}^{13}/\chi_B^2$  ratios. It is to be noted that, the baryon-charge correlations ( $\chi_{BQ}^{13}/\chi_B^2$ ) in Figs. 2 and 4 show non-monotonic behavior as a function of  $\sqrt{s_{NN}}$  could be due to baryon to meson dominated freeze-out of the system [32]. The different energy dependence be-

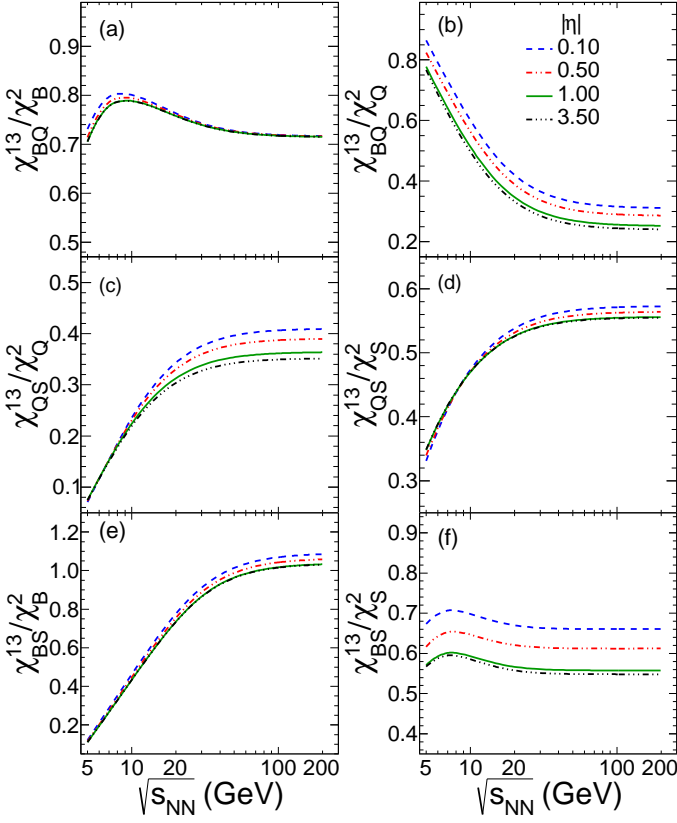


FIG. 4: Ratios of off-diagonal susceptibility to second order susceptibility ( $\chi_{xy}^{13}/\chi_{x,y}^2$ ) as a function of  $\sqrt{s_{NN}}$  within  $0.2 \leq p_T$  GeV/c  $\leq 2.0$  from the HRG model, where  $x$  and  $y$  stand for either  $B$ ,  $Q$  or  $S$ . Panels (a) and (b) shows the off-diagonal susceptibility ratios for charged baryons. Panels (c) and (d) shows the off-diagonal susceptibility ratios for charged particles with at least one strange quark. Panels (e) and (f) shows the off-diagonal susceptibility ratios for baryons with strange quark. The ratios are also compared for various  $\eta$  acceptance ranges.

havior between  $\chi_{BQ}^{11}/\chi_B^2$  and  $\chi_{BQ}^{13}/\chi_B^2$  is primarily due to contribution from resonances with higher electric charge (in particular  $\Delta^{++}$ ).

For completeness, we have also studied the ratios of  $\chi^{31}/\chi^2$  as a function of collision energies. Figure 5 shows the  $\sqrt{s_{NN}}$  dependence of  $\chi_{QS}^{31}/\chi_Q^2$ ,  $\chi_{BQ}^{31}/\chi_Q^2$ ,  $\chi_{BQ}^{31}/\chi_B^2$ ,  $\chi_{QS}^{31}/\chi_S^2$ ,  $\chi_{BS}^{31}/\chi_B^2$ , and  $\chi_{BS}^{31}/\chi_S^2$  for two different  $p_T$  and  $\eta$  acceptances. These susceptibility ratios are different from the  $\chi^{13}/\chi^2$  ratios since we take the third derivative of the first conserved quantity. The effect will be more if the first considered conserved number is electric charge or strangeness.

### C. Effect of different conserved charged states

Experimentally it is difficult to measure all the baryons or strange particles produced in the collisions. Hence, we

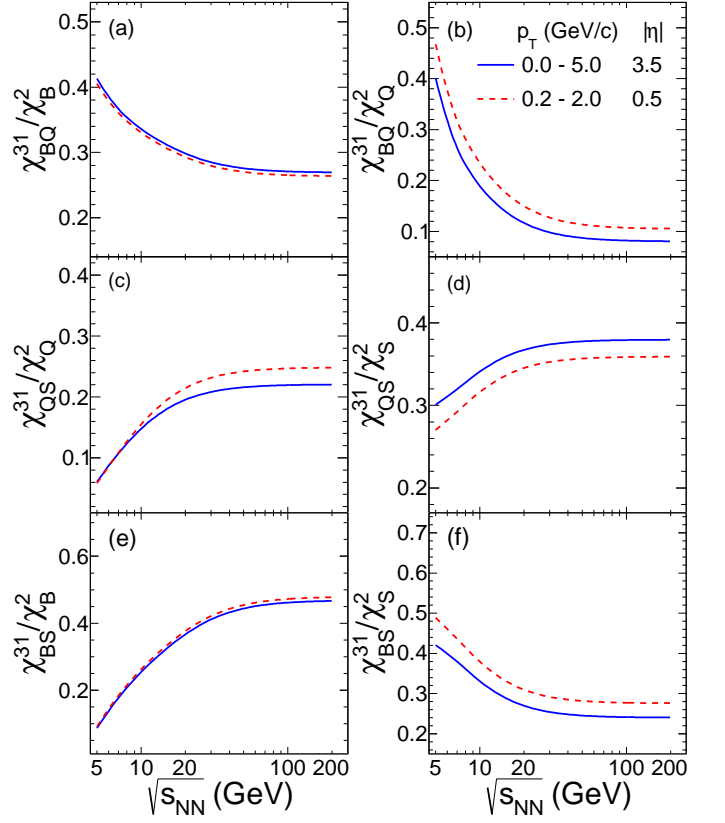


FIG. 5: Ratios of off-diagonal susceptibility to second order susceptibility ( $\chi_{xy}^{31}/\chi_{x,y}^2$ ) as a function of  $\sqrt{s_{NN}}$  for full  $p_T$  and  $|\eta|$  acceptance, and within  $0.2 \leq p_T$  GeV/c  $\leq 2.0$  with  $|\eta| \leq 0.5$  from the HRG model, where  $x$  and  $y$  stand for either  $B$ ,  $Q$  or  $S$ . Panels (a) and (b) shows the off-diagonal susceptibility ratios for charged baryons. Panels (c) and (d) shows the off-diagonal susceptibility ratios for charged particles with at least one strange quark. Panels (e) and (f) shows the off-diagonal susceptibility ratios for baryons with strange quark.

have not considered the correlated susceptibilities related to strange baryons ( $\chi_{BS}$ ). Further, in the denominator we need to take the susceptibilities of  $\chi_p$  and  $\chi_K$  for protons (anti-protons) and kaons (anti-kaons), respectively, which may act as a proxy for baryons and strange particles. Figure 6 shows the variation of  $\chi_{BQ}^{11}/\chi_p^2$ ,  $\chi_{BQ}^{13}/\chi_p^2$ ,  $\chi_{QS}^{11}/\chi_K^2$  and  $\chi_{QS}^{13}/\chi_K^2$  ratios as a function of  $\sqrt{s_{NN}}$  for various charge states. In case of baryon charge correlations ( $\chi_{BQ}$ ) only charged baryons (anti-baryons) contribute, starting from proton to higher mass charged baryons. For each of the cases, the  $\chi_{BQ}$  are compared with the inclusion of higher charge states. There is significant difference in  $\chi_{BQ}^{11}/\chi_p^2$  and  $\chi_{BQ}^{13}/\chi_p^2$  after inclusion of higher charge states like  $\Delta^{++}$ . Since all the baryons have baryon number 1, only the baryons with higher electric charge number contribute to the increase of baryon charge correlations. Similarly, for strange electric charge correlations ( $\chi_{QS}$ ) only charged strange par-

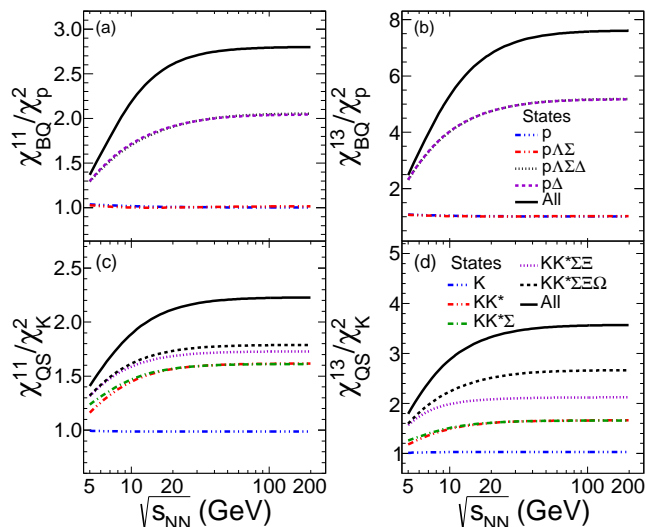


FIG. 6: The variation of  $\chi_{BQ}^{11,13}/\chi_p^2$  and  $\chi_{QS}^{11,13}/\chi_K^2$  as a function of  $\sqrt{s_{NN}}$  within  $0.2 \leq p_T$  (GeV/c)  $\leq 2.0$  and  $|\eta| \leq 0.5$ . Panels (a) and (b) shows the susceptibility ratios for charged baryon and panels (c) and (d) shows the susceptibility ratios charged particles with strangeness content. Also shown are the comparison of effect of inclusion of particles with higher charge or strangeness states to the susceptibility ratios. The proton and kaon susceptibilities in the denominator are from the primordial production.

ticles contribute starting from kaon and higher mass charged strange particles. There is a strong dependence of  $\chi_{QS}^{11}/\chi_K^2$  and  $\chi_{QS}^{13}/\chi_K^2$  on the inclusion of higher order strange charged states.

The measured proton (anti-proton) and kaon (anti-kaon) have contributions from primordial production as well as from resonance decay. We have studied the resonance decay effect on the mixed susceptibility ratios by taking the resonance contribution in the denominator ( $\chi_p$  and  $\chi_K$ ). The resonance decay contributions to the proton and kaon susceptibilities are estimated as discussed in [33, 34]. Figure 7 shows the collision energy dependence of  $\chi_{BQ}^{11}/\chi_p^2$ ,  $\chi_{BQ}^{13}/\chi_p^2$ ,  $\chi_{QS}^{11}/\chi_K^2$  and  $\chi_{QS}^{13}/\chi_K^2$  ratios for different charged states. The denominators  $\chi_p^2$  and  $\chi_K^2$  have contributions from primordial as well as resonance decay. The numerators have contributions from primordial particles and without decay of resonances. The  $\chi_{BQ}^{11}/\chi_p^2$  in Fig. 6 and Fig. 7 show different energy dependence because of the resonance decay contributions to the protons in the denominator for Fig. 7. Further, the baryon-charge correlation  $\chi_{BQ}^{11}/\chi_p^2$  and  $\chi_{BQ}^{13}/\chi_p^2$  (case all) in Fig. 6 show different energy dependence compared to the  $\chi_{BQ}^{11}/\chi_B^2$  in Fig. 3 and  $\chi_{BQ}^{13}/\chi_B^2$  in Fig. 4. This difference in the ratios arise due to the difference in  $\chi^2$  for protons and baryons. The  $\chi^2$  of the baryons is always higher than the  $\chi^2$  of protons and also has an energy dependence.

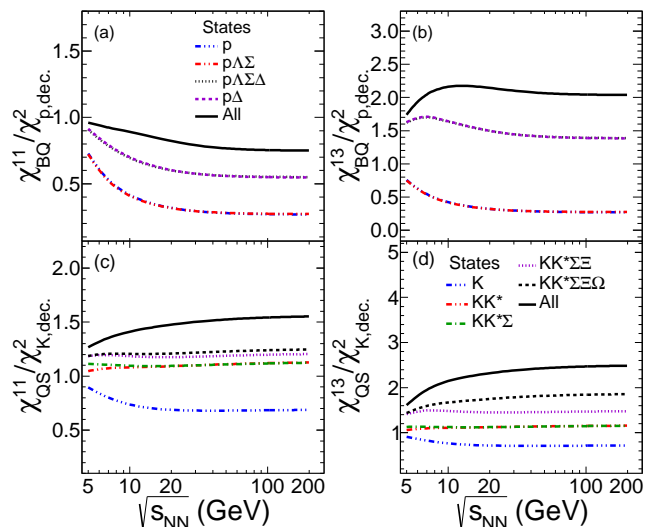


FIG. 7: The variation of  $\chi_{BQ}^{11,13}/\chi_p^2$  and  $\chi_{QS}^{11,13}/\chi_K^2$  as a function of  $\sqrt{s_{NN}}$  within  $0.2 \leq p_T$  (GeV/c)  $\leq 2.0$  and  $|\eta| \leq 0.5$ . Panels (a) and (b) shows the susceptibility ratios for charged baryon and panels (c) and (d) shows the susceptibility ratios charged particles with strangeness content. Also shown are the comparison of effect of inclusion of particles with higher charge or strangeness states to the susceptibility ratios. The proton and kaon susceptibilities in the denominator are from the primordial as well as resonance decay contributions.

#### IV. BASELINE FOR CRITICAL FLUCTUATIONS

In order to locate the critical point in the QCD phase diagram, one may compare the experimentally measured cumulants of multiplicity distributions with the theoretical model predictions. These theoretical models, without any phase transition (non-CEP), may provide a baseline contribution to the measured cumulants from data. As proposed in [21], there are different combinations of cumulants of protons and pions which are independent of QCD based coupling parameters. Some of such cumulant ratios are :  $(\kappa_{3p}\kappa_{2\pi}^{3/2})/(\kappa_{3\pi}\kappa_{2p}^{3/2})$ ,  $(\kappa_{4p}\kappa_{2\pi}^2)/(\kappa_{4\pi}\kappa_{2p}^2)$ ,  $(\kappa_{4p}^3\kappa_{3\pi}^4)/(\kappa_{4\pi}^3\kappa_{3p}^4)$ ,  $\kappa_{2p2\pi}^2/(\kappa_{4p}\kappa_{4\pi})$  and  $\kappa_{2p1\pi}^3/(\kappa_{3p}^2\kappa_{3\pi})$ . Where,  $\kappa_{nx}$  are the cumulants of different order with  $n = 1, 2, 3, 4$  and  $x$  being the proton or pion. In case of non-interacting particles in the classical Boltzmann regime, in the absence of critical fluctuations, the fluctuations of particle number follow Poisson statistics. Hence, after subtracting the Poisson contribution from the above cumulant ratios, one can predict the contributions of critical fluctuations in the cumulant ratios. These subtracted cumulant ratios will be at 1 in the proximity of the critical point. However, keeping in mind that the experimental measurements are performed within a finite kinematic acceptance and can accept only a fraction of particles, the HRG model based baseline will be a better substitute compared to Poisson expectations. We have esti-

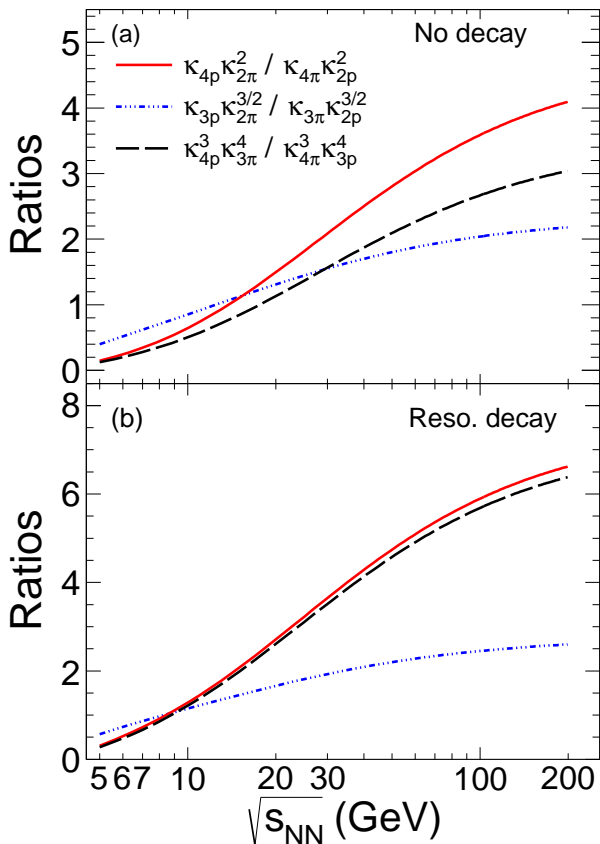


FIG. 8: Various cumulant ratios of proton and pion as a functions of  $\sqrt{s_{NN}}$  within  $0.2 \leq p_T$  GeV/c  $\leq 2.0$  and  $|\eta| \leq 0.5$ . The upper panel (a) shows for the primordial proton and pion production, the lower panel (b) shows the proton and pion production from primordial and resonance decay contributions.

mated the baseline for the above cumulant ratios using the HRG model, which will give the thermal contribution to the cumulant ratios. The first two ratios are the ratios of the skewness and kurtosis of protons and pions, where skewness =  $\kappa_3/\kappa_2^{3/2}$  and kurtosis =  $\kappa_4/\kappa_2^2$ . The last two ratios involve mixed cumulants of protons and pions. In the HRG model, there is no interaction between the particles, hence the contribution of mixed cumulants will be zero. Figure 8 shows the first three ratios, defined above, as a function  $\sqrt{s_{NN}}$ . The upper panel of Fig. 8 shows the different cumulant ratios by taking primordial pions and protons, the lower panel show the cumulant ra-

tios of protons and pions which have contributions from both primordial as well as resonance decay. These ratios are calculated using the HRG model should and can be considered as baseline instead of Poisson contribution as baseline.

## V. SUMMARY

In summary, keeping in mind the importance of mixed susceptibilities and pion-proton cumulants in unraveling the phase structure of QCD, we have provided the variation of these observables as a function of colliding beam energy within the ambit of a HRG model. The results presented in this paper will provide the required baseline for the corresponding measurements in the experiments.

We have studied the effect of experimental acceptance on the ratios of the mixed susceptibilities using a hadron resonance gas model. We have considered  $\chi_{BQ}^{11}/\chi_B^2$ ,  $\chi_{BQ}^{11}/\chi_Q^2$ ,  $\chi_{QS}^{11}/\chi_Q^2$ ,  $\chi_{QS}^{11}/\chi_S^2$ ,  $\chi_{BS}^{11}/\chi_B^2$  and  $\chi_{BS}^{11}/\chi_S^2$  ratios, which have contributions from charged baryons (anti-baryons), charged strange or baryon strange particles. There is a small dependence on  $p_T$  and  $\eta$  for the above susceptibility ratios. However, there is a strong energy dependence for all the ratios. These susceptibility ratios are very sensitive to the different charge states. In a real experimental situation, it is difficult to measure the strange baryons ( $\Lambda^0$  and higher masses strange baryons) on an event-by-event basis and calculate their cumulants for fluctuations, specially at lower beam energies. Instead we have concentrated on measurable ratios like  $\chi_{BQ}^{11}/\chi_p^2$ ,  $\chi_{BQ}^{13}/\chi_p^2$ ,  $\chi_{QS}^{11}/\chi_K^2$  and  $\chi_{QS}^{13}/\chi_K^2$  and presented the HRG expectations for primordial and resonance decay contributions.

We have also provided a HRG based calculation of realistic baseline (non-CEP expectation) for a set of new observables recently proposed for critical fluctuations using the different combinations of cumulant ratios of protons and pions [21]. The experimentally measured values of these ratios, after subtraction of the non-CEP contributions, are expected to be at unity in presence of CEP. These cumulant ratios of proton and pion from the HRG model calculations are observed to increase as a function of  $\sqrt{s_{NN}}$ . These ratios calculated using the HRG model should be used as baseline instead of Poisson expectation for the interpretation of data related to QCD critical point.

**ACKNOWLEDGEMENT:** BM acknowledges support from DST, DAE and SERB projects.

[1] M. A. Stephanov, K. Rajagopal and E. V. Shuryak, Phys. Rev. Lett. **81**, 4816 (1998).  
 [2] M. G. Alford, K. Rajagopal and F. Wilczek, Phys. Lett. B **422**, 247 (1998).  
 [3] Y. Aoki, G. Endrodi, Z. Fodor, S. D. Katz and K. K. Szabo, Nature **443**, 675 (2006).

[4] M. Asakawa, U. W. Heinz and B. Muller, Phys. Rev. Lett. **85**, 2072 (2000).  
 [5] M. Asakawa, S. Ejiri and M. Kitazawa, Phys. Rev. Lett. **103**, 262301 (2009).  
 [6] M. A. Stephanov, Prog. Theor. Phys. Suppl. **153**, 139 (2004); Int. J. Mod. Phys. A **20**, 4387 (2005).

- [7] M. M. Aggarwal *et al.* [STAR Collaboration], Phys. Rev. Lett. **105**, 022302 (2010).
- [8] L. Adamczyk *et al.* [STAR Collaboration], Phys. Rev. Lett. **112**, 032302 (2014).
- [9] L. Adamczyk *et al.* [STAR Collaboration], Phys. Rev. Lett. **113**, 092301 (2014).
- [10] A. Adare *et al.* [PHENIX Collaboration], Phys. Rev. C **93**, 011901 (2016).
- [11] S. Gupta, X. Luo, B. Mohanty, H. G. Ritter and N. Xu, Science **332**, 1525 (2011).
- [12] A. Bazavov *et al.* [HotQCD Collaboration], Phys. Rev. D **86**, 034509 (2012).
- [13] R. V. Gavai and S. Gupta, Phys. Rev. D **65**, 094515 (2002).
- [14] V. Koch, A. Majumder and J. Randrup, Phys. Rev. Lett. **95**, 182301 (2005).
- [15] A. Majumder and B. Muller, Phys. Rev. C **74**, 054901 (2006).
- [16] R. V. Gavai and S. Gupta, Phys. Rev. D **73**, 014004 (2006).
- [17] A. Bazavov, H. T. Ding, P. Hegde, O. Kaczmarek, F. Karsch, E. Laermann, S. Mukherjee and P. Petreczky *et al.*, Phys. Rev. Lett. **109** (2012) 192302.
- [18] S. Borsanyi, Z. Fodor, S. D. Katz, S. Krieg, C. Ratti and K. Szabo, JHEP **1201**, 138 (2012).
- [19] M. A. Stephanov, K. Rajagopal and E. V. Shuryak, Phys. Rev. D **60**, 114028 (1999).
- [20] Z. Fodor and S. D. Katz, JHEP **0404**, 050 (2004).
- [21] C. Athanasiou, K. Rajagopal and M. Stephanov, Phys. Rev. D **82**, 074008 (2010).
- [22] M. A. Stephanov, Phys. Rev. Lett. **102**, 032301 (2009).
- [23] R. V. Gavai and S. Gupta, Phys. Lett. B **696**, 459 (2011).
- [24] M. Cheng, P. Hegde, C. Jung, F. Karsch, O. Kaczmarek, E. Laermann, R. D. Mawhinney and C. Miao *et al.*, Phys. Rev. D **79**, 074505 (2009).
- [25] M. A. Stephanov, Phys. Rev. Lett. **107** (2011) 052301.
- [26] P. Braun-Munzinger, K. Redlich and J. Stachel, In \*Hwa, R.C. (ed.) et al.: Quark Gluon Plasma 3, 491–599 (2004).
- [27] J. Cleymans, H. Oeschler, K. Redlich and S. Wheaton, Phys. Rev. C **73**, 034905 (2006).
- [28] A. Andronic, P. Braun-Munzinger, K. Redlich and J. Stachel, J. Phys. G **38**, 124081 (2011).
- [29] P. Garg, D. K. Mishra, P. K. Netrakanti, B. Mohanty, A. K. Mohanty, B. K. Singh and N. Xu, Phys. Lett. B **726**, 691 (2013).
- [30] F. Karsch, K. Morita and K. Redlich, Phys. Rev. C **93**, no. 3, 034907 (2016).
- [31] F. Karsch and K. Redlich, Phys. Lett. B **695** 136 (2011).
- [32] H. Oeschler, J. Cleymans, K. Redlich and S. Wheaton, J. Phys. G **32**, S223 (2006).
- [33] D. K. Mishra, P. Garg, P. K. Netrakanti and A. K. Mohanty, Phys. Rev. C **94**, 014905 (2016).
- [34] M. Nahrgang, M. Bluhm, P. Alba, R. Bellwied and C. Ratti, Eur. Phys. J. C **75**, no. 12, 573 (2015).